PHYSICAL REVIEW C **78**, 061602(R) (2008)

Determination of the ^{233}Pa(n, f) reaction cross section from 11.5 to 16.5 MeV neutron energy by the hybrid surrogate ratio approach

B. K. Nayak,[1] A. Saxena,[1] D. C. Biswas,[1] E. T. Mirgule,[1] B.V. John,[1] S. Santra,[1]
R. P. Vind,[1] R. K. Choudhury,[1] and S. Ganesan[2]
[1]*Nuclear Physics Division, Bhabha Atomic Research Centre, Mumbai-400085, India*
[2]*Reactor Physics Design Division, Bhabha Atomic Research Centre, Mumbai- 400085, India*
(Received 5 August 2008; published 12 December 2008)

A new hybrid surrogate ratio approach has been employed to determine neutron-induced fission cross sections of ^{233}Pa in the energy range of 11.5 to 16.5 MeV for the first time. The fission probability of ^{234}Pa and ^{236}U compound nuclei produced in ^{232}Th(^{6}Li, α)^{234}Pa and ^{232}Th(^{6}Li, d)^{236}U transfer reaction channels has been measured at $E_{\rm lab} = 38.0$ MeV in the excitation energy range of 17.0 to 22.0 MeV within the framework of the absolute surrogate method. The ^{233}Pa(n, f) cross sections are then deduced from the measured fission decay probability ratios of ^{234}Pa and ^{236}U compound nuclei using the surrogate ratio method. The ^{233}Pa(n, f) cross section data from the present experiment along with the data from the literature, covering the neutron energy range of 1.0 to 16.5 MeV have been compared with the predictions of statistical model code EMPIRE-2.19. While the present data are consistent with the model predictions, there is a discrepancy between the earlier experimental data and EMPIRE-2.19 predictions in the neutron energy range of 7.0 to 10.0 MeV.

DOI: 10.1103/PhysRevC.78.061602 PACS number(s): 24.50.+g, 24.75.+i, 25.85.Ec, 28.20.−v

Determination of the neutron-induced fission cross sections of short-lived actinide nuclei is a major challenge for nuclear physics and nuclear astrophysics. Often indirect methods such as the surrogate reaction method involving a stable target and projectile are employed to estimate the compound nuclear cross sections for short-lived target nuclei. In the past, direct-reaction-fission correlation measurements have been used to get indirect estimates of reaction cross sections of many compound systems in the actinide region that are unavailable for neutron-induced fission reactions because of the lack of target material with suitable lifetimes [1–4]. In the earlier studies, surrogate reaction methods were used in the simplest form, where measured fission probabilities were simply multiplied by estimated neutron compound capture cross sections to deduce the (n, f) cross section. Comparison with cases in which (n, f) cross sections had been measured directly indicated that this technique could yield estimated (n, f) cross sections with accuracy of order 10–20% for incident neutron energies above 1.0 MeV. More recently, the surrogate ratio method [5,6] has been employed to deduce (n, f) cross sections, whereby one is able to remove most of the systematic uncertainties present in the measurements in applying the simple surrogate reaction method. The surrogate ratio method has the advantage that the dependence on J^{π} disappears for the excitation energy higher than 8.0 MeV, and the ratio method is shown to be insensitive to pre-equilibrium effects for (n, f) reactions [5]. Hence the applicability of the surrogate reaction ratio method is more relevant for excitation energies higher than 8.0 MeV.

The basic nuclear data of the ^{233}Pa(n, f) reaction in the thorium-uranium fuel cycle is of topical interest in connection with an accelerator-driven system (ADS) for nuclear power generation and transmutation of nuclear waste [7,8]. The primary reaction of importance in the thorium cycle is the one producing the fissile nucleus ^{233}U from neutron capture on ^{232}Th. The net production of ^{233}U is controlled by the 27 day half-life of the ^{233}Pa isotope. As this isotope is produced in an intermediate step during the formation of the fissile ^{233}U nucleus, reactions competing with its natural decay affect the production rate of the fissile fuel. In a thermal reactor, neutron capture of ^{233}Pa is totally dominating, but the situation is different in a fast reactor system such as the ADS. At fast neutron energies, the fission cross section increases and the capture cross section decreases. Thus, in this type of system, the magnitude of the fission cross section becomes a key parameter, which must be known with some precision. The accuracy with which the $n + ^{233}$Pa fission cross section is needed for fast breeding reactors and ADSs has been estimated to be less than 20% [9].

There is only one direct neutron energy resolved ^{233}Pa(n, f) cross section measurement which has been carried out with quasimonoenergetic neutrons, where the ^{3}H(p, n)^{3}He and ^{2}H(^{2}H, n)^{3}He reactions were used to produce neutrons with energies of $E_n = 1.0$–3.8 MeV and $E_n = 5.0$–8.5 MeV, respectively [10,11]. The limited experimental data on direct measurement could be explained by the short half-life of ^{233}Pa. To overcome these problems, the surrogate reaction technique has also been used [12] to measure the fission probability of ^{234}Pa formed in the reaction ^{232}Th(^{3}He, p)^{234}Pa. The neutron-induced fission cross sections for the $n + ^{233}$Pa reaction have then been deduced from the product of this experimentally determined fission probability with the compound nucleus cross section determined from optical model calculations in the equivalent neutron energy range from threshold to 10.0 MeV [12]. None of these experimental data on ^{233}Pa(n, f) cross sections in the energy range 6.0 to 10.0 MeV match the recommended values for the neutron-induced capture and fission cross sections extracted from the ENDF/B-VII.0 [13] and JENDL-3.3 [14] data evaluations.

As of today, there is no experimental measurement of the ^{233}Pa(n, f) cross section beyond 10.0 MeV neutron energy. The experimental data beyond 10 MeV is of importance for

hybrid fusion-fission systems and for the ADS [8]. It can also give a stringent test to the neutron-induced capture and fission cross sections extracted from various evaluations. In the present work, we have employed a new hybrid surrogate ratio approach involving aspects of both the absolute and ratio surrogate methods to derive ^{233}Pa(n, f) cross sections from measurements of the ratio of the fission decay probabilities of ^{234}Pa and ^{236}U compound nuclei over the excitation energy range of 17.0 to 22.0 MeV. These nuclei are formed in ^{232}Th(^{6}Li, α)^{234}Pa and ^{232}Th(^{6}Li, d)^{236}U transfer reaction channels, respectively. The present measurement is unique in that the two compound residues are formed in situ in the same experiment with an overlapping excitation energy spectrum, which has helped us to employ the surrogate ratio method to extract the ^{233}Pa(n, f) cross section. The ground state Q values (Q_{gg}) for ^{232}Th(^{6}Li, α)^{234}Pa and ^{232}Th(^{6}Li, d)^{236}U transfer reactions are 6.77 and −6.05 MeV, respectively. Hence the ^{234}Pa and ^{236}U compound systems can be populated at overlapping excitation energies in ^{6}Li + ^{232}Th transfer reactions for bombarding energies around 36.0 MeV.

The surrogate ratio method has been described in Refs. [5,6]. Here we describe in brief the formalism and the essential steps adopted by us. In the earlier work [5,6,15], two compound nuclei used in the ratio method were formed using the same direct reaction with two different targets. In the present work, using a single target the compound nuclei, ^{234}Pa and ^{236}U are formed in situ in two different direct reactions ^{232}Th(^{6}Li, α)^{234}Pa and ^{232}Th(^{6}Li, d)^{236}U, respectively. Using the same target to populate two compound systems eliminates the uncertainty due to the target thickness. The projectile-like fragment (PLF) singles and coincidence between PLF and fission fragment measurements were carried out to determine the fission decay probabilities of the ^{236}U and ^{234}Pa compound nuclei produced in the transfer reactions within the framework of the absolute surrogate method by dividing the number of PLF-fission coincidences ($N_{\alpha_i - f}$) by associated PLF-singles (N_{α_i}) data as follows:

$$\Gamma_f^{\mathrm{CN}}(E_{\mathrm{ex}}) = \frac{N_{\alpha_i - f}}{N_{\alpha_i}}, \tag{1}$$

where α_i denotes the α or deuteron PLF channel corresponding to the ^{234}Pa or ^{236}U compound nucleus. The relative fission probabilities of the compound nuclei are multiplied with the relative neutron-induced corresponding surrogate reaction compound nuclear formation cross sections of $\sigma^{\mathrm{CN}}_{n+^{233}\mathrm{Pa}}$ and $\sigma^{\mathrm{CN}}_{n+^{233}\mathrm{U}}$ to obtain the ratio of the compound nuclear reaction cross section at the same excitation energies of $n + {}^{233}\mathrm{Pa} \rightarrow {}^{234}\mathrm{Pa} \rightarrow$fission and $n + {}^{235}\mathrm{U} \rightarrow {}^{236}\mathrm{U} \rightarrow$fission reactions as follows:

$$\frac{\sigma_f^{n+^{233}\mathrm{Pa}\rightarrow^{234}\mathrm{Pa}}(E_{\mathrm{ex}})}{\sigma_f^{n+^{235}\mathrm{U}\rightarrow^{236}\mathrm{U}}(E_{\mathrm{ex}})} = R(E_{\mathrm{ex}}) = \frac{\sigma^{\mathrm{CN}}_{n+^{233}\mathrm{Pa}}(E_{\mathrm{ex}})}{\sigma^{\mathrm{CN}}_{n+^{235}\mathrm{U}}(E_{\mathrm{ex}})} \frac{\Gamma_f^{^{234}\mathrm{Pa}}(E_{\mathrm{ex}})}{\Gamma_f^{^{236}\mathrm{U}}(E_{\mathrm{ex}})}. \tag{2}$$

The $n + {}^{235}\mathrm{U} \rightarrow {}^{236}\mathrm{U} \rightarrow$fission cross section, which is well measured, has been used as the reference monitor to determine the $n + {}^{233}\mathrm{Pa} \rightarrow {}^{234}\mathrm{Pa} \rightarrow$fission cross section from the $R(E_{\mathrm{ex}})$ measurement. This is a new hybrid surrogate approach, which involves aspects of both the absolute and ratio surrogate methods.

A self-supporting thorium target of thickness 2.0 mg/cm^2 was bombarded with a ^{6}Li beam of energy $E_{\mathrm{lab}} = 38.0$ MeV from a 14 MV Pelletron accelerator at Mumbai. A solid state ΔE-E telescope of thickness 150.0 μm to 1.0 mm was kept at $\theta_{\mathrm{lab}} = 90^\circ$ with respect to the beam direction around the transfer grazing angle to identify the PLFs. A 16 strip solid state detector (each strip of size 2.0 × 64.0 mm) was placed at a back angle covering the laboratory angular range of 141°–158° to detect fission fragments in coincidence with PLFs. The ratios of the coincidence to single counts for ^{232}Th(^{6}Li, α)^{234}Pa and ^{232}Th(^{6}Li, d)^{236}U reaction channels were determined as a function of excitation energy. The time correlation between PLFs and fission fragments are recorded through a time-to-amplitude converter (TAC). The correlation between fission fragment pulse height and TAC is shown in Fig. 1.

The ratio of coincidence to single counts corresponds to the fission decay probability of the compound systems formed in the transfer reaction. The ΔE and E silicon detectors were energy calibrated by measuring elastic scattering at different energies and angles. The proton, deuteron, triton, α, and ^{6}Li particles are uniquely identified by plotting ΔE against the total energy $\Delta E + E_{\mathrm{res}}$. This plot was transformed to create an effective particle identification (PI) versus energy plot, which was generated using the linearization function (PI $= b(E_{\mathrm{tot}}^{1.95} - E^{1.95-})$, where E_{tot} is the total particle energy, E is the energy deposited in the E detector, and b is a constant.

Figure 2 shows a typical PI versus energy curve for the PLF telescope. The PI parameter has been zoomed to show p, d, t, and α PLFs clearly, therefore the elastic channel has gone out of the scale and is not shown in Fig. 2. The excitation energy spectra of the target-like residues of ^{234}Pa and ^{236}U were determined by employing two-body kinematics for ^{4}He and deuteron PLF channels. The excitation energy spectra so obtained for ^{234}Pa and ^{236}U nuclei are shown in Fig. 3. The excitation energy spectra obtained for PLF-fission fragment

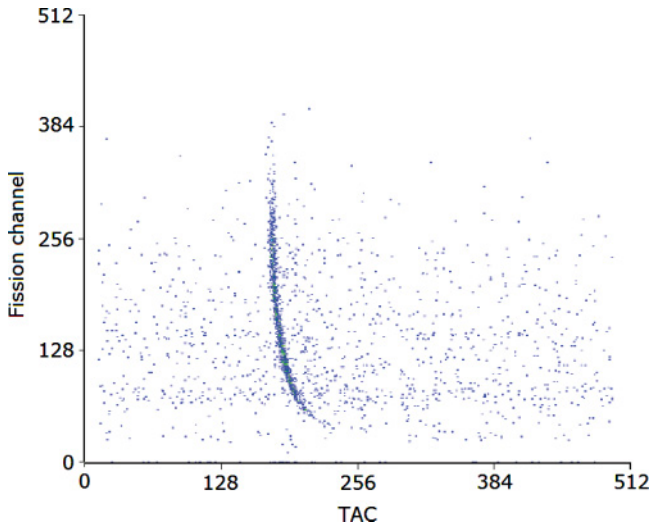

FIG. 1. (Color online) Fission fragment pulse height vs coincidence TAC between PLFs and fission fragments.

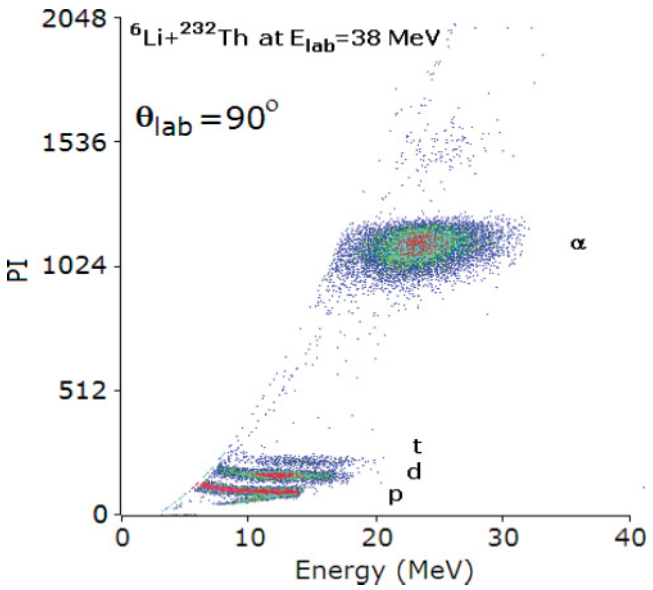

FIG. 2. (Color online) Particle identification plot for ^{6}Li + ^{232}Th at $E_{\rm lab}$ = 38 MeV.

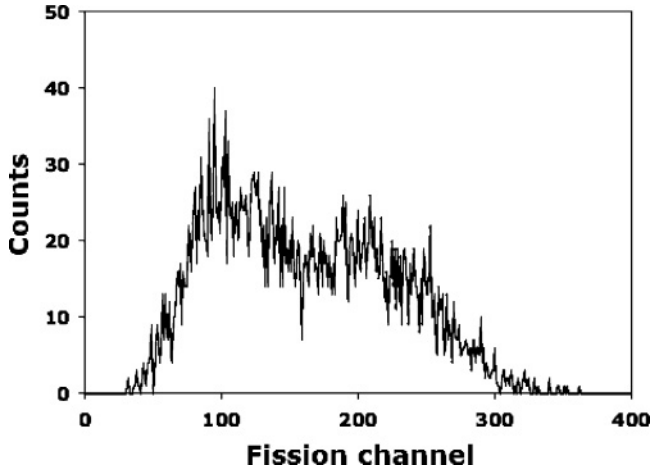

FIG. 4. Typical fission spectrum obtained in coincidence with PLF.

coincidence are also shown in the same figure. A typical fission fragment spectrum in coincidence with α and deuteron PLFs is shown in Fig. 4. The ratio of coincidence to singles counts were determined in steps of 1.0 MeV excitation energy bins in the excitation energy range 17.0–22.0 MeV for ^{234}Pa and ^{236}U nuclei.

For each excitation energy bin, the ratio of fission decay probability of ^{234}Pa to ^{236}U was determined. The n + ^{235}U → ^{236}U → fission reaction cross section was the reference monitor and taken from ENDF/B-VII.0 [13]. The neutron

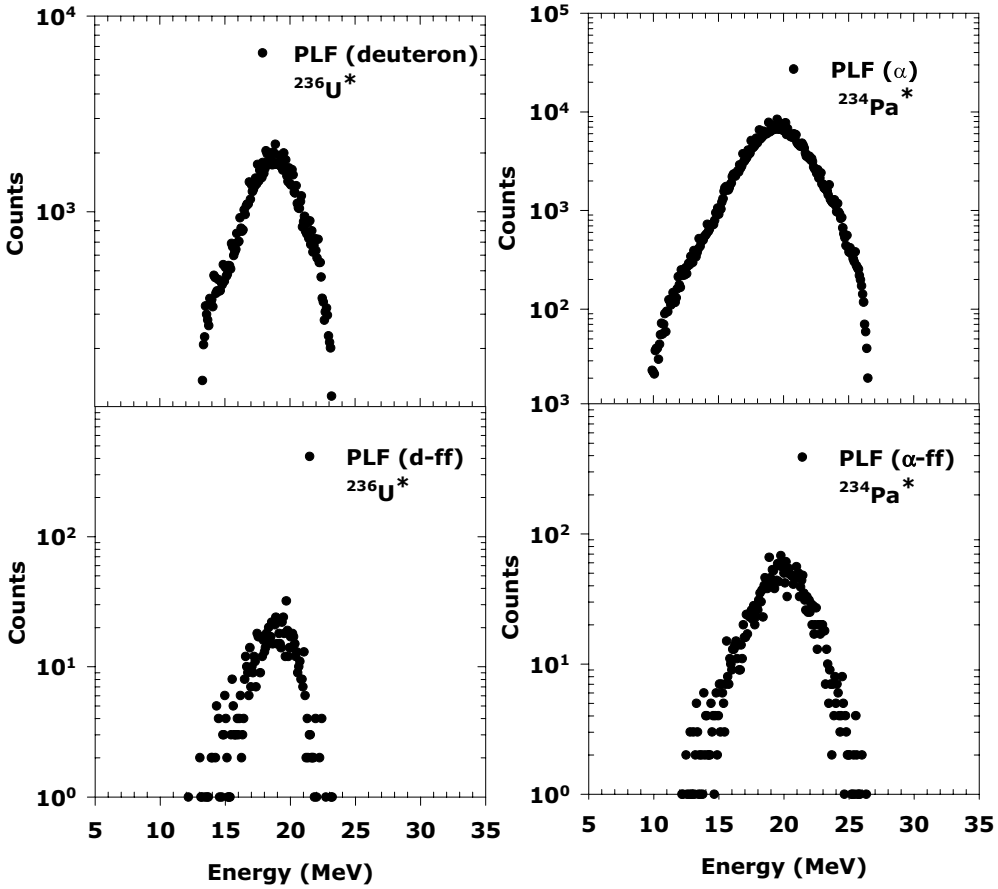

FIG. 3. Excitation energy spectra of targetlike fragments in ^{6}Li + ^{232}Th reaction with (bottom) and without (upper) coincidence with fission fragments.

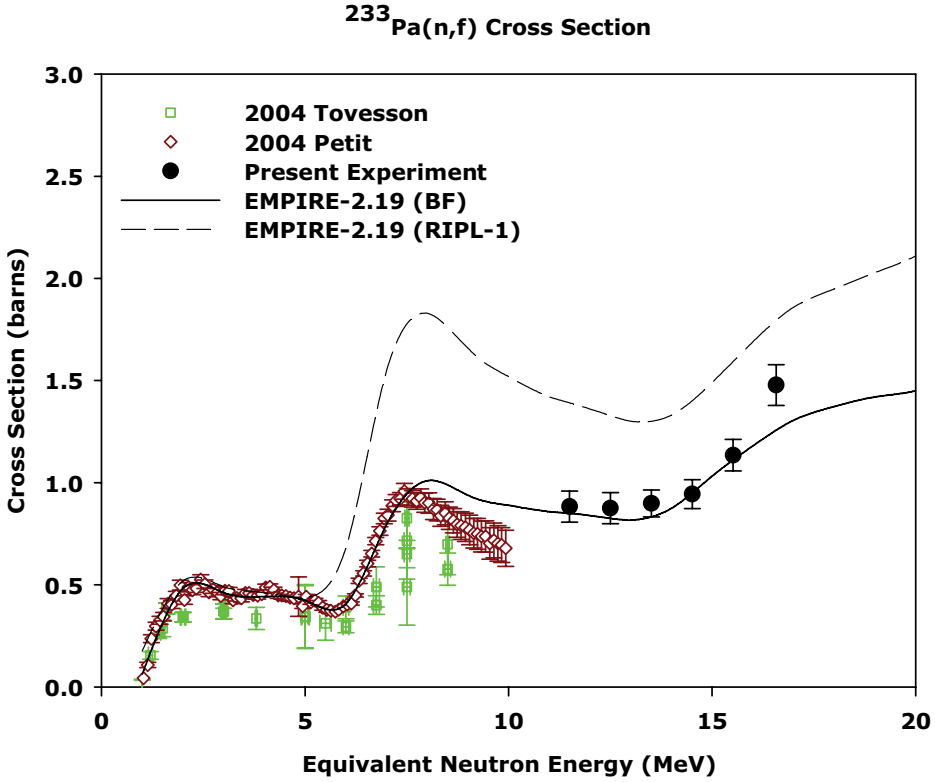

FIG. 5. (Color online) Experimental ^{233}Pa(n, f) cross section and calculated results using the EMPIRE-2.19 code.

capture cross sections were calculated by the EMPIRE-2.19 code [16] for ^{235}U and ^{233}Pa nuclei in the excitation energy range 17.0–22.0 MeV. Using Eqs. (1) and (2), the ^{233}Pa(n, f) cross sections as a function of excitation energy of ^{233}Pa were obtained over the excitation energy range 17.0–22.0 MeV. The excitation energy was scaled down to the equivalent neutron energy range of 11.5–16.5 MeV by subtracting the neutron separation energy of ^{233}Pa($S_n = 5.45$ MeV).

The EMPIRE-2.19 calculations were also performed to quantitatively understand the ^{233}Pa(n, f) cross sections over the neutron energy of 1.0–16.5 MeV for various sets of fission barrier parameters available from evaluations. EMPIRE-2.19 specific level densities were used, which include the Fermi gas formalism and BCS pairing at low energies. Here the excitation energy dependence of the shell correction in the level density parameter was included as given by Ignatyuk *et al.* [17]. The asymptotic values of level density parameters are derived from systematics that include the effects of deformation, spin, and vibration enhancement factors. The EMPIRE-2.19 code uses the RIPL-2 set of input parameters which are an outcome of a coordinated research program of the International Atomic Energy Agency [18,19]. The RIPL-2 library contains nuclear masses, deformations, matter densities, discrete levels and decay schemes, spacing of neutron resonances, optical model potentials, level density parameters, giant resonance parameters, γ-ray strength functions, and fission barriers. We have used the exciton model [20] for including preequilibrium emission. In the present case, equilibrium emission is treated by the Hauser-Feshbach theory in EMPIRE-2.19. The fission cross sections predicted by RIPL-2 fission barriers do not agree with experimental data at all energies.

However, if one uses the fission barrier given by RIPL-1, where the fission barrier parameters are those compiled by Maslov [21] for post-thorium systems, the calculated cross sections give good agreement with experimental data at low energies, but there is a significant disagreement at higher energies as shown in Fig. 5. We also carried out an EMPIRE-2.19 analysis using the fission barrier heights obtained from the barrier formula (BF) [22] which was fitted to reproduce the fission barriers given by Bjornholm and Lynn [23]. This barrier formula is based on the Hugenholtz and Van Hove theorem [24] for many-body theory in infinite matter added with finite size effects such as the Coulomb, surface, asymmetry, and pairing terms. The fission barrier heights corresponding to various isotopes used in the EMPIRE-2.19 calculations for RIPL-1, RIPL-2, and the barrier formula are listed in Table I. The prediction of EMPIRE-2.19 using fission barrier heights obtained from BF compared reasonably well with the experimental data. It is, however, observed that by increasing the ^{233}Pa inner barrier height from the 5.9 MeV

TABLE I. Fission barrier heights used in EMPIRE-2.19 calculations for RIPL-1, RIPL-2, and the barrier formula (BF).

System	Inner barrier height (MeV)			Outer barrier height (MeV)		
	RIPL-1	RIPL-2	BF	RIPL-1	RIPL-2	BF
^{234}Pa	6.3	5.4	6.2	6.2	5.3	6.4
^{233}Pa	5.7	4.7	6.2	5.8	6.0	6.3
^{232}Pa	5.0	4.7	6.2	6.4	5.9	6.2
^{231}Pa	5.5	4.1	5.9	5.5	5.8	6.1

BF predicted value to 6.2 MeV, a better comparison of the EMPIRE-2.19 prediction with the experimental data is obtained, as shown in Fig. 5 as a continuous line. It is seen that there are still some discrepancies between the model prediction and experimental data in the excitation energy range of 7.0–10.0 MeV.

In summary, we have employed a new hybrid surrogate ratio approach, which involves aspects of both the absolute and ratio methods in a unique way to determine the ^{233}Pa(n, f) cross sections in the equivalent neutron energy range of 11.5 to 16.5 MeV using ^{6}Li + ^{232}Th transfer-fission correlation measurements. The ^{234}Pa and ^{236}U compound systems have been populated at overlapping excitation energies in the same experiment through ^{232}Th(^{6}Li, α)^{234}Pa and ^{232}Th(^{6}Li, d)^{236}U transfer channels at $E_{\rm lab}$ = 38 MeV, and the absolute surrogate method is used to determine fission decay probabilities of the above compound nuclei by dividing the number of PLF-fission coincidences by the associated PLF-singles data. The experimental values of fission decay probability ratios of ^{234}Pa and ^{236}U compound nuclei at the same excitation energy have been used to deduce the ^{233}Pa(n, f) cross sections using a surrogate ratio approach. Present experimental data on ^{233}Pa(n, f) reaction cross sections along with the data from the literature covering the equivalent neutron energy range 1.0–16.5 MeV have been compared with the predictions of EMPIRE-2.19 for fission barrier heights corresponding to RIPL-1, RIPL-2, and the barrier formula. The ^{233}Pa(n, f) cross section data are well reproduced by EMPIRE-2.19 calculations by using fission barrier heights given by the barrier formula [22]. However, the discrepancies between EMPIRE-2.19 predictions and the experimental data observed in the energy range 7.0–10.0 MeV require further investigation.

The authors thank Dr. S. Kailas for discussions and his keen interest in the present work. The authors also acknowledge Drs. S. Mukherjee, S. S. Godre, R. K. Jain, Y. K. Gupta, Appanna Babu, P. Desai, and V. K. Pandya, for their helpful discussions and support during the experiment.

[1] J. D. Cramer and H. C. Britt, Phys. Rev. C **2**, 2350 (1970).
[2] H. C. Britt and J. D. Cramer, Phys. Rev. C **2**, 1758 (1970).
[3] J. Escher, L. Ahle, L. Bernstein, J. A. Church, F. Dietrich, C. Forss'en, and R. Hoffman, Nucl. Phys. **A758**, 86c (2005).
[4] F. S. Dietrich and J. E. Escher, Nucl. Phys. **A787**, 237 (2007).
[5] C. Plettner *et al*., Phys. Rev. C **71**, 051602(R) (2005).
[6] J. T. Burke *et al*., Phys. Rev. C **73**, 054604 (2006).
[7] C. Rubbia *et al*., Conceptual Design of a Fast Neutron Operated High Power Energy Amplifier, CERN Report No. CERN/AT/95-44(ET), 1995.
[8] S. Ganesan, Pramana J. Phys. **68**, 257 (2007).
[9] V. G. Pronyaev, "Summary Report of the Consultants' Meeting on Assessment of Nuclear Data Needs for Thorium and Other Advanced Cycles," IAEA Report No. INDC(NDS)-408 (1999).
[10] F. Tovesson, F. J. Hambsch, A. Oberstedt, B. Fogelberg, E. Ramstrom, and S. Oberstedt, Phys. Rev. Lett. **88**, 062502 (2002).
[11] F. Tovesson *et al*., Nucl. Phys. **A733**, 3 (2004).
[12] M. Petit *et al*., Nucl. Phys. **A735**, 345 (2004).
[13] M. B. Chadwick *et al*., Nucl. Data Sheets **107**, 2931 (2006).
[14] K. Shibata *et al*., J. Nucl. Sci. Technol. **39**, 1125 (2002) .
[15] V. F. Weisskopf and P. H. Ewing, Phys. Rev. **57**, 472 (1940).
[16] M. Herman, R. Capote, B. V. Carlson, P. Oblozinský, M. Sin, A. Trkov, H. Wienke, and V. Zerkin, Nucl. Data Sheets **108**, 2655 (2007).
[17] A. V. Ignatyuk, G. N. Smirenkin, and A. S. Tishin, Yad. Fiz **21**, 485 (1995) [Sov. J. Nucl. Phys. **21**, 255 (1975)].
[18] Nuclear Model Parameters Testing with Nuclear Data Evaluation Reference Input Parameter Library: Phase II, INDC-431, edited by M. Hermann (April 2002); see the website: http://www-nds.indcentre.org.in/RIPL-2/home.html.
[19] A. Mamdouh *et al*., Nucl. Phys. **A644**, 389 (1998); **A679**, 337 (2001).
[20] E. Betak and P. Oblozonsky, Report INDC (SLK)-001, IAEA, Vienna (1993).
[21] V. M. Maslov, RIPL-1 Handbook, TEXDOC-000, IAEA, Vienna (1998).
[22] S. K. Gupta and A. Saxena, in Proceedings of 8th Korean Nuclear Data Workshop, Pohang, 25–26 August 2005.
[23] S. Bjornholm and J. E. Lynn, Rev. Mod. Phys. **52**, 725 (1980).
[24] N. H. Hugenholtz and W. Van Hove, Physica (Utrecht) **24**, 363 (1958).